IEEE Access
Multidisciplinary | Rapid Review | Open Access Journal

Received 24 January 2024, accepted 13 February 2024, date of publication 19 February 2024, date of current version 26 February 2024.

*Digital Object Identifier 10.1109/ACCESS.2024.3367356*

RESEARCH ARTICLE

# Smartwatch-Based Kinematic Walking Direction Estimation Using Paired Principal Component Analysis

**JAE WOOK PARK[1], JAE HONG LEE[1], (Student Member, IEEE), JUNU PARK[1], AND CHAN GOOK PARK[2], (Member, IEEE)**

[1]Department of Aerospace Engineering, Automation and Systems Research Institute, Seoul National University, Seoul 08826, South Korea
[2]Department of Aerospace Engineering, Institute of Advanced Aerospace Technology, Seoul National University, Seoul 08826, South Korea

Corresponding author: Chan Gook Park (chanpark@snu.ac.kr)

This work was supported in part by Samsung Electronics Company Ltd., through the Mobile eXperience (MX) under Grant 0418-20220065.

**ABSTRACT** The dynamic behavior of pedestrians causes a misalignment problem between the sensor orientation and the walking direction, which hinders the performance of pedestrian dead reckoning (PDR) systems. Pedestrians wearing smartwatches are constantly faced with this problem when running. In this paper, we propose a novel kinematic modeling of arm swing that segments arm swing motion from the movement of the center of mass of the body. The proposed decomposition method allows for effective negation of the sensor outputs due to the redundant motion that obstructs the estimation of the true walking direction. The correct direction vector is computed by deducting the direction vector of the arm swing from that of the entire motion, which are both derived from performing two separate principal component analyses (PCA). The performance of the proposed method was evaluated through several experiments. In the running track experiment, the proposed method demonstrates the best performance, with 57% – 70% performance improvement compared to the existing methods. In the general scenario involving both walking and running, the proposed method outperforms the baseline method by 56%, improving the generality of the PCA-based methods.

**INDEX TERMS** Gait kinematics, inertial sensors, pedestrian dead reckoning (PDR), principal component analysis (PCA), smartwatch, walking direction estimation.

## I. INTRODUCTION

Pedestrian localization stands as a fundamental technology for services based on the location of pedestrians [1], [2], [3]. Recently, services that provide the trajectory for people exercising with wearable devices have gained attention. While outdoor localization systems relying on global navigation satellite system (GNSS) have been widely commercialized [4], they face limitations when multi-path phenomena occur in urban areas [5] and require external infrastructure such as satellites. In addition, indoor localization systems that utilize Wi-Fi [6], [7], [8], Ultra-Wide Band (UWB) [9], Bluetooth [10], and RFID [11] have been studied, but they also require pre-installed infrastructure.

Therefore, pedestrian localization methods that do not rely on infrastructure have been continuously researched, and the most representative one is pedestrian dead reckoning (PDR) [12]. In an inertial sensor-based PDR system, the current position is estimated recursively using the step length and the walking direction. Between the two parameters, the latter poses a greater importance in achieving an accurate pedestrian localization [13].

Generally, the attitude and heading reference systems (AHRS) have been mainly used for walking direction estimation [14], [15], [16], [17]. However, these algorithms assume that the direction pointed by the sensor aligns with the

The associate editor coordinating the review of this manuscript and approving it for publication was Mauro Fadda.

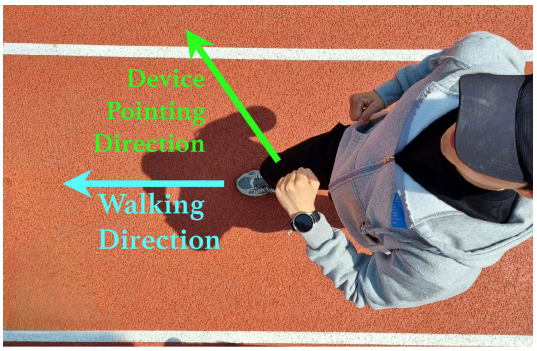


**FIGURE 1.** Directional misalignment between the direction pointed by the sensor and the actual walking direction of the pedestrian.

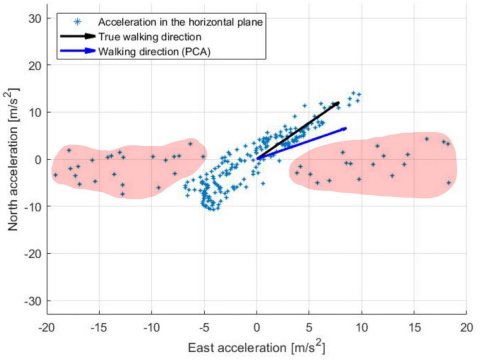


**FIGURE 2.** The impact of non-forward acceleration, represented by the red area, in the PCA-based methods.

actual walking direction of the pedestrian. This assumption is not appropriate in situations where the two directions are inconsistent as shown in Fig. 1. Moreover, this misalignment often occurs in PDR where pedestrians wear sensors on their hands or wrists. Various studies have been conducted to address this problem [18], [19], [20], [21], [22], [23], [24], [25], [26], [27], [28], [29], [30], [31], [32] and one of the most popular methods is the principal component analysis (PCA)-based method.

The PCA-based methods estimate the walking direction by performing a PCA on the distribution of the acceleration measurements from a few steps of walking, resulting in the estimation of the actual walking direction of the pedestrian [18], [19], [20]. However, previous studies in [33], [34], and [35] have highlighted that the effectiveness of the PCA-based methods diminishes when the distribution includes acceleration components that do not align with the walking direction. This problem is prevalent during running, as depicted in Fig. 1, where the swing motions of the arms deviate from the walking direction, leading to an increase in the estimation error.

In this paper, we propose a solution to this problem by first calculating the direction vectors of the entire motion and the swing motion of the arms using two PCAs, hence from the title: paired PCA. Furthermore, by modeling the swing motion of the arms, we eliminate the movements that do not correspond to the true walking direction, thereby enhancing the accuracy and stability of the walking direction estimation.

The contributions of this paper can be summarized as follows.

1) Analysis on human motion is performed, aiming to decompose the intricate movements into two categories: those that yield acceleration components aligned with the walking direction and those that do not.
2) A novel method of eliminating the influence of misaligned acceleration components is proposed. The method utilizes paired PCA to derive direction vectors from both the acceleration and the angular rate measurements, which are then combined with kinematic modeling of the arm swing.
3) Comprehensive experiments, including a running-only sequence, on pedestrians wearing smartwatches are conducted. The evaluation shows that our method outperforms the existing methods in estimating an accurate walking direction.

The paper is organized as follows. Section II provides an overview of existing studies on walking direction estimation. In Section III, an analysis of human motion is conducted. Building upon the insights gained from Section III, Section IV proposes a novel method for estimating walking direction by decomposing human motion through the modeling of arm swing. Section V presents experimental results and performance validation of the proposed method. Finally, Section VI suggests conclusions of this study.

## II. RELATED WORKS

Inertial sensor-based walking direction estimation methods can be divided into two main approaches: analyzing the primary components and modeling the human gait characteristics. Recently, methods incorporating neural networks have also been investigated [27].

One of the representative methods that analyze the primary components is the method that utilizes the acceleration measured during walking [19]. This method operates under the assumption that the direction that maximizes the variance of the acceleration distribution is consistent with the actual walking direction of the pedestrian. The method performs PCA on the projected acceleration onto the navigation frame or the horizontal plane. However, this method implies limitations in its assumption. As pointed out in [33], the inclusion of non-forward acceleration, i.e., accelerations that are not aligned with the walking direction, undermines the assumption of this method, resulting in a degradation of the estimation performance as shown in Fig. 2. As mentioned in Section I, this concern is a critical limitation of the PCA-based methods since it is a problem that persists even in ordinary running situations.

Another method for analyzing the primary components is to use the angular rate measured during walking [32]. This method introduces a constraint that the angular rate in the walking direction should be zero, based on the intuition that

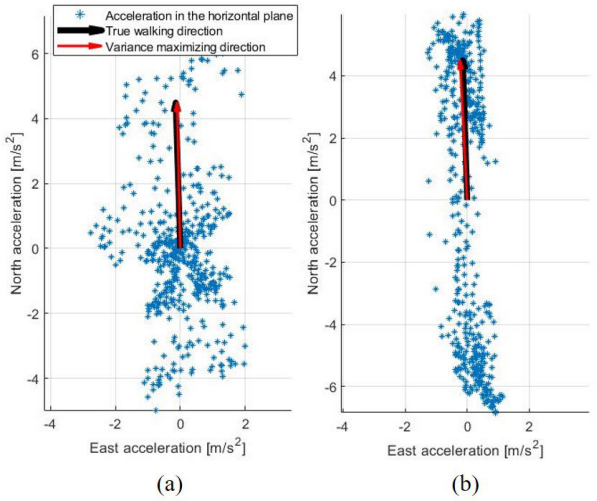


**FIGURE 3.** Distribution of acceleration with inertial sensors attached to (a) the center of mass of the body while walking and (b) the wrist while swinging an arm as if walking.

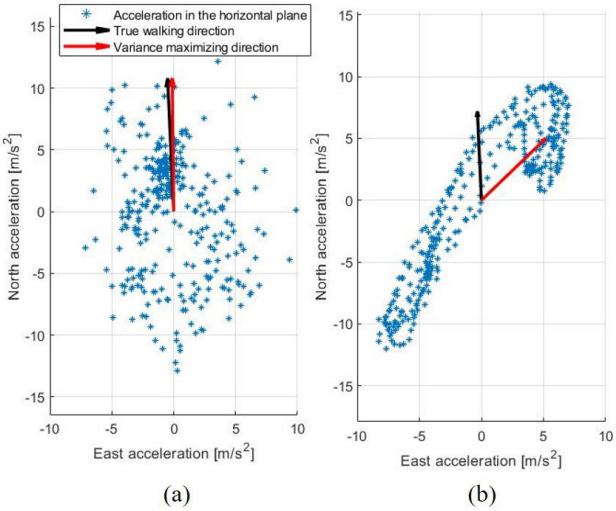


**FIGURE 4.** Distribution of acceleration with inertial sensors attached to (a) the center of mass of the body while running and (b) the wrist while swinging an arm as if running.

the swing of the arms or legs is aligned with the walking direction. However, if the swing direction is no longer aligned with the walking direction, the estimated direction will deviate from the actual walking direction. As there is no guarantee that the swing and walking direction will be aligned, this can be considered as a limitation of this method.

As for the approach of modeling human gait characteristics, a method introduces a kinematic modeling of the acceleration measured during walking. The key idea underlying this method, proposed by Leonardo et al. [24], is that the acceleration of the center of mass of the pedestrian during walking follows a rolling-foot model [36]. Unlike other methods, they emphasize the strengths of their method, which does not require step detection, has no 0°/180° ambiguity, does not require algorithm customization depending on users, and does not rely on the pre-trained model. However, the rolling-foot model loses its validity if the sensor is not positioned at the center of mass of the pedestrian. As they mentioned, when holding the sensor in the hand and swinging, the performance of the method is degraded.

Another method for modeling gait characteristics is to model acceleration measured during walking as a Gaussian mixture [30]. This method, called WAlking direction estimation based on Inertial Signal Statistics (WAISS), considers that the distribution of the acceleration measurements can be characterized with two Gaussian distributions, each representing the frontal and the lateral acceleration. This method consists of two phases. In the training phase, a Gaussian mixture model (GMM) is constructed using the Expectation-Maximization (EM) algorithm. In the subsequent walking direction estimation phase, the direction that maximizes the log-likelihood of the GMM is deemed as the walking direction. However, this method requires a pre-trained model, which may vary depending on the individual and the motion, and thus, the key lies in creating a personalized and sophisticated model [35].

Our proposed method combines two main approaches: one that analyzes the primary components and one that models human gait characteristics, specifically the difference in arm swing patterns between walking and running. The former approach actively utilizes the intrinsic features of the inertial measurements but does not exploit the characteristics of human gaits, and vice versa for the latter approach. Our method integrates the strengths of both approaches and mitigates their limitations by employing PCAs on the inertial measurements, and also incorporating kinematic modeling of arm swing.

## III. HUMAN MOTION ANALYSIS

Walking and running are the most basic human behavior. During walking, a person alternates their feet while synchronously moving their arms to maintain balance [37]. Humans repeat these cyclic movements while walking and running. Humans can also raise their arms to look at the watch, wave their hands and so on while walking, but for the purpose of this paper, these possibilities are excluded and only normal walking is considered. In the context of wearing an inertial sensor on the wrist during these motions, the sensor output reflects a combination of the center of mass motion and arm swing. To empirically validate this intuitive understanding and gain a deeper knowledge of human gaits, a series of experiments was conducted. A detailed description of the experimental setup can be found in Section V.

Intuitively speaking, humans tend to swing their arms in a back-and-forth manner rather than diagonally when walking. In Fig. 3(a), the distribution of acceleration is shown when the inertial sensor is attached to the center of mass of the body (chest) during several steps of walking. Fig. 3(b) shows the distribution of acceleration when the inertial sensor is attached to the wrist while the participant stands still but only swings the arm as if were walking to exclude the effect of the body transition. It is shown that the variance maximizing

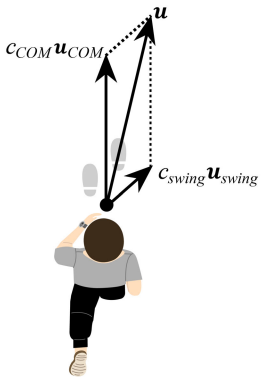


**FIGURE 5.** Schematic diagram of each direction vector during running.

direction of Fig. 3(a) and that of Fig. 3(b) both coincide with the true walking direction. This finding substantiates our initial intuition that the direction of the center of mass of the body and the direction of arm swing align during walking.

Unfortunately, the outcomes are different for running. Fig. 4(a) presents the distribution of the acceleration measured with an inertial sensor attached to the center of mass of the body (chest) during running. Fig. 4(b) shows the distribution of the acceleration measured with an inertial sensor attached to the wrist while the participant stands still but only swings the arm as if were running to exclude the effect of the body movement.

In this case, the variance maximizing direction of Fig. 4(a) aligns with the true walking direction, while that of Fig. 4(b) no longer coincides with the true walking direction. That is, when humans run, as depicted in Fig. 1, the arm swing occurs in a "diagonal" manner with the arms held closer to the body [38], deviating from the true walking direction, unlike in walking. While the acceleration components generated by the movement of the center of mass of the body provide valuable cues for estimating the true walking direction, the acceleration components generated by the arm swing consequently impede accurate estimation due to their misalignment. With continued arm swings, the distribution of acceleration measured with inertial sensor on the wrist while running would be somewhat skewed compared to Fig. 4(a).

Starting this section, we stated that the most basic human motion is walking and running. However, even in the case of running, the skewing of the acceleration distribution occurs due to the influence of arm swing-induced acceleration components. As mentioned in Section II, these acceleration components have been identified as a critical limitation of the PCA-based methods. Our analysis on the human motion decomposition serves as the motivation of our research, and we hence aim to establish a broader applicability of the PCA-based methods.

## IV. PEDESTRIAN WALKING DIRECTION ESTIMATION USING MOTION DECOMPOSITION

The fundamental concept of our proposed method is based on the premise that human motion is comprised of two distinct components: the movement associated with the center of mass (COM) of the body and the swing of the arms, as elucidated in Section III. Thus, the problem can be defined as follows.

$$\boldsymbol{u} = c_{COM}\boldsymbol{u}_{COM} + c_{swing}\boldsymbol{u}_{swing} \tag{1}$$

where $c$ and $\boldsymbol{u}$ represent the coefficient and the unit direction vector, respectively, whereas the subscripts $COM$ and $swing$ represent the motion of the center of mass of the body and the arm swing, respectively.

The ultimate goal of the proposed method is to determine the walking direction through an accurate estimation of $\boldsymbol{u}_{COM}$, of which the direct calculation is unfeasible as the inertial sensor is attached to the wrist, not to the center of mass of the body. Fig. 5 provides a conceptual illustration of the direction vectors in the human running motion, depicting how $\boldsymbol{u}$ is comprised of both $\boldsymbol{u}_{COM}$ and $\boldsymbol{u}_{swing}$.

### A. DERIVATION OF THE DIRECTION VECTOR OF THE ENTIRE MOTION

The unit vector $\boldsymbol{u}$ is derived from $\hat{\theta}$, which is the direction that maximizes the variance of the distribution of the acceleration measurements from a few steps. $\hat{\theta}$ is estimated through performing PCA as follows.

$$\hat{\theta} = \arg\max_{\theta}\left(\sum_{i=1}^{M}(\boldsymbol{\beta}\cdot\boldsymbol{a}^n(i))^2\right) \tag{2}$$

$$\boldsymbol{u} = \left[\cos\hat{\theta}\ \sin\hat{\theta}\right]^T \tag{3}$$

where $\boldsymbol{\beta} = \left[\cos\theta\ \sin\theta\right]$, $\boldsymbol{a}^n$ is the acceleration measurement in the north-east plane of the navigation frame($n$), and $M$ is the number of data samples generated in a few steps. However, as discussed in Section III, the direction vector $\boldsymbol{u}$ includes the arm swing, and hence cannot represent the true walking direction: the direction of the center of mass.

However, PCA alone still leaves with 0°/180° ambiguity of the estimated direction vector, meaning the forward and backward walking along the $\hat{\theta}$ direction line cannot be distinguished. To resolve this ambiguity, we leverage the angular rate measurements [19]. The forward and backward swings are differentiated using the sign of the angular rate of the axis orthogonal to the swing. Then, the chronological order of the acceleration measurements of the forward swing reveals the "forward" direction.

### B. DERIVATION OF THE DIRECTION VECTOR OF THE ARM SWING

The vector $\boldsymbol{u}_{swing}$ is derived from the angular rate measurements. When humans swing their arms while moving, the arms rotate around an axis orthogonal to the swing direction. As a result, the angular rates corresponding to the orthogonal axis exhibit relatively larger values, while the angular rates along the swing direction display relatively smaller values [32]. Exploiting this swing characteristic, the unit vector $\boldsymbol{u}_{swing}$ is derived from $\hat{\theta}_{swing}$, which is the direction that minimizes the variance of the distribution of the angular

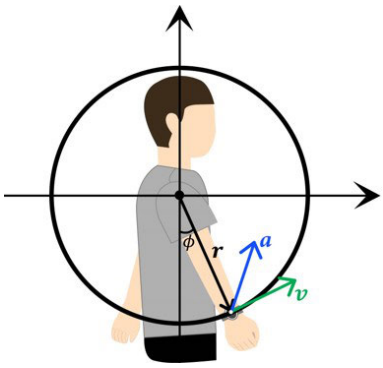


**FIGURE 6.** Kinematic modeling of arm swing motion.

rate measurements from a few steps. $\hat{\theta}_{swing}$ is estimated through performing PCA as follows.

$$\hat{\theta}_{swing} = \arg\min_{\theta}(\sum_{i=1}^{M}(\boldsymbol{\beta}\cdot\boldsymbol{\omega}^n(i))^2) \tag{4}$$

$$\boldsymbol{u}_{swing} = \left[\cos\hat{\theta}_{swing}\ \sin\hat{\theta}_{swing}\right]^T \tag{5}$$

where $\boldsymbol{\omega}^n$ is the angular rate measurement in the north-east plane of the navigation frame.

### C. DERIVATION OF THE COEFFICIENTS WITH KINEMATIC MODELING OF ARM SWING

The coefficients $c_{COM}$ and $c_{swing}$, which are multiplied with each direction vector in (1), are defined in this subsection. Based on the analysis in Section III, the following assumption can be derived.

$$\boldsymbol{a}^n = \boldsymbol{a}^n_{COM} + \boldsymbol{a}^n_{swing} \tag{6}$$

where $\boldsymbol{a}^n_{COM}$ and $\boldsymbol{a}^n_{swing}$ are the acceleration in the navigation frame due to the movement of the center of mass of the body and the arm swing, respectively.

From (6), the coefficient $c_{swing}$ is defined as the proportion of $\boldsymbol{a}^n_{swing}$ in $\boldsymbol{a}^n$. The definition of the coefficient $c_{swing}$ can be expressed as the following equation.

$$c_{swing} = \frac{\Sigma_i^M ||\boldsymbol{a}^n_{swing}(i)||_2}{\Sigma_i^M ||\boldsymbol{a}^n(i)||_2} \tag{7}$$

where $M$ is the number of data samples generated over several swing cycles, and $||\cdot||_2$ denotes the $l^2$-norm of a vector. $\boldsymbol{a}^n$ is already known from the acceleration measurement, but $\boldsymbol{a}^n_{swing}$ is not directly known and has to be found through modeling. From (1), $\boldsymbol{u}$ is a unit vector, hence the following relation can be derived. The detailed derivation of (8) is presented in the Appendix.

$$c_{COM} + c_{swing} \approx 1. \tag{8}$$

The arm swing is a periodic circular motion around a specific point in the shoulder and primarily occurs within a specific plane. Therefore, we model the swing of the arm as a two-dimensional circular motion of an object, as shown in Fig. 6. In polar coordinates, the position of an object in two-dimensional circular motion is as follows.

$$\boldsymbol{r} = r\hat{\boldsymbol{r}} \tag{9}$$

where $r$ is the radial distance between the object and the origin and $\hat{\boldsymbol{r}}$ is the unit vector along the radial direction from the origin to the object. The velocity of an object is the time derivative of (9).

$$\boldsymbol{v} = \frac{d}{dt}\boldsymbol{r} = \frac{dr}{dt}\hat{\boldsymbol{r}} + r\frac{d\hat{\boldsymbol{r}}}{dt} = \frac{dr}{dt}\hat{\boldsymbol{r}} + r\omega\hat{\boldsymbol{\phi}} \tag{10}$$

where $\hat{\boldsymbol{\phi}}$ is the time-varying unit vector associated with the changing $\phi$, $\phi$ is the angle between the vertical axis and the radial line from the origin to the object, and $\omega$ is the magnitude of the angular rate of the object. Differentiating (10) once more with respect to time, the acceleration of an object in two-dimensional circular motion in polar coordinates can be derived as follows.

$$\boldsymbol{a} = \frac{d}{dt}\boldsymbol{v} = (\frac{d^2r}{dt^2} - r\omega^2)\hat{\boldsymbol{r}} + (2\frac{dr}{dt}\omega + r\frac{d\omega}{dt})\hat{\boldsymbol{\phi}}. \tag{11}$$

The first term on the right-hand side of (11) represents the centripetal acceleration, while the second term represents the tangential acceleration. Consequently, (11) serves as the kinematic model of $\boldsymbol{a}^n_{swing}$.

From a physical perspective, $r$ represents the distance between a specific point on the shoulder and the location where the sensor is attached, so we assume $\frac{dr}{dt} = 0$. Also, since the Cartesian coordinates $\hat{\boldsymbol{x}}$ and $\hat{\boldsymbol{y}}$ can be represented in polar coordinates as $\hat{\boldsymbol{r}} = \cos\phi\ \hat{\boldsymbol{x}} + \sin\phi\ \hat{\boldsymbol{y}}$ and $\hat{\boldsymbol{\phi}} = -\sin\phi\ \hat{\boldsymbol{x}} + \cos\phi\ \hat{\boldsymbol{y}}$, we can simplify $\boldsymbol{a}^n_{swing}$ as follows.

$$\begin{aligned}\boldsymbol{a}^n_{swing} = &(-r\omega^2\cos\phi - r\frac{d\omega}{dt}\sin\phi)\hat{\boldsymbol{x}} \\ &+ (-r\omega^2\sin\phi + r\frac{d\omega}{dt}\cos\phi)\hat{\boldsymbol{y}}.\end{aligned} \tag{12}$$

Hence, $||\boldsymbol{a}^n_{swing}||_2$ can be determined using the following expression:

$$||\boldsymbol{a}^n_{swing}||_2 = r\sqrt{\omega^4 + \left(\frac{d\omega}{dt}\right)^2}. \tag{13}$$

As indicated by (7), the final expression for $c_{swing}$ is derived as:

$$c_{swing} = \frac{\Sigma_i^M \left(r\sqrt{\omega(i)^4 + \left(\frac{d\omega(i)}{dt}\right)^2}\right)}{\Sigma_i^M ||\boldsymbol{a}^n(i)||_2} \tag{14}$$

where $\omega$ is the magnitude of the angular rate measurement and $||\boldsymbol{a}^n||_2$ is the magnitude of the acceleration measurement

**TABLE 1. Test user profile.**

| Test User | Height [cm] | Age | Gender | $r$* [m] |
|---|---|---|---|---|
| Subject1 | 174 | 27 | male | 0.35 |
| Subject2 | 177 | 26 | male | 0.35 |
| Subject3 | 167 | 31 | male | 0.30 |
| Subject4 | 163 | 24 | female | 0.30 |
| Subject5 | 159 | 34 | female | 0.30 |
| Subject6 | 185 | 28 | male | 0.40 |

* $r$: assumed linear distance from the shoulder to the smartwatch

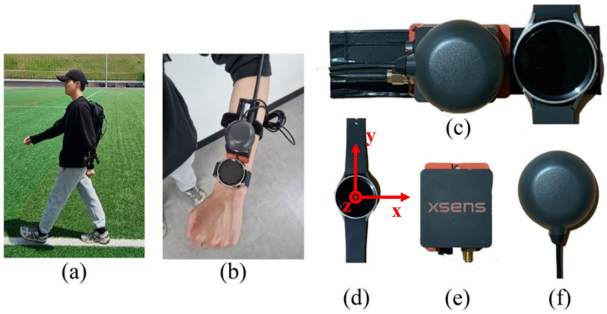


**FIGURE 7. (a) Participant wearing experimental equipment (b) Experimental setup worn on the left wrist (c) A smartwatch, MTi-680G, and antenna mounted on the platform (d) Smartwatch (e) MTi-680G (f) Antenna for GNSS information acquisition.**

in the navigation frame. Additionally, considering the relationship presented in (8), we can obtain $c_{COM}$ as follows.

$$c_{COM} = 1 - \frac{\Sigma_i^M \left( r \sqrt{\omega(i)^4 + \left( \frac{d\omega(i)}{dt} \right)^2} \right)}{\Sigma_i^M ||\boldsymbol{a}^n(i)||_2}. \tag{15}$$

### D. WALKING DIRECTION ESTIMATION

Finally, as the objective of the proposed method is to estimate the direction vector of the center of mass of the body, $\boldsymbol{u}_{COM}$, we rearrange (1) as follows:

$$\boldsymbol{u}_{COM} = \frac{1}{c_{COM}} \boldsymbol{u} - \frac{c_{swing}}{c_{COM}} \boldsymbol{u}_{swing}. \tag{16}$$

Using (16) along with (3), (5), (14) and (15), we can eventually estimate $\boldsymbol{u}_{COM}$ while eliminating the influence of the arm swing, isolating the acceleration components associated with the center of mass of the body.

## V. EXPERIMENTS AND RESULTS

To assess the performance of the proposed method, we conducted three experiments. The first experiment aims to validate the rationality of the swing modeling by estimating the coefficients for various motions. The second experiment is a running-only scenario that serves to quantitatively evaluate the proposed method in comparison with the existing methods. In the third experiment, we conduct a comprehensive evaluation of both the proposed method

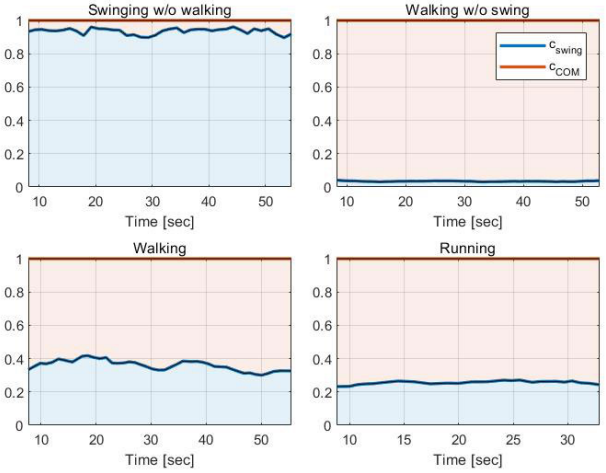


**FIGURE 8. Cumulative estimates of $c_{swing}$ and $c_{COM}$.**

**TABLE 2. Estimation of the coefficient for each motion.**

| | $c_{swing}$ | | | |
|---|---|---|---|---|
| | Swinging w/o walking | Walking w/o swinging | Walking | Running |
| Mean | 0.94 | 0.03 | 0.36 | 0.26 |
| Std | 0.02 | 0.01 | 0.03 | 0.01 |
| Min | 0.90 | 0.03 | 0.30 | 0.23 |
| Max | 0.96 | 0.04 | 0.42 | 0.27 |

and the existing methods in a more general scenario. The compared methods include:

1) The PCA-based method, Rotation Matrix and PCA (RMPCA) [19]: This method utilizes PCA and shares similarities with the proposed method in terms of exploiting the characteristics of the acceleration distribution. Thus, it serves as a baseline method;
2) The Least Square-based Method (LSM) [32];
3) WAlking direction estimation based on Inertial Signal Statistics (WAISS) [30].

### A. EXPERIMENTAL SETUP

Six participants engaged in natural walking while wearing a Samsung Galaxy Watch 5 Pro, XSens MTi-680G, and antenna on a platform on their left wrist. Information regarding the participants involved in the experiments is presented in Table 1. The experimental setup of the participant with the devices is shown in Fig. 7. The smartwatch outputs acceleration, angular rate, magnetism, and barometric pressure at 100Hz. Among these raw data, we utilized the x, y, and z-axis acceleration and angular rate. The three axes of the smartwatch, x, y, and z, are shown in Fig. 7(d). Each measurement is stored on the smartwatch in the form of a CSV file, and after the experiment, the smartwatch is directly connected to a laptop to transfer the CSV file to the laptop. On the laptop, our algorithm implemented in MATLAB works and processes the measurements in the

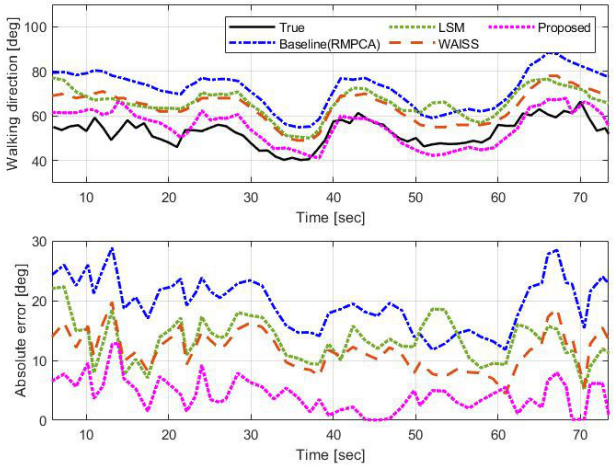


**FIGURE 9.** Estimated walking direction and estimation error for subject1 in running track experiment.

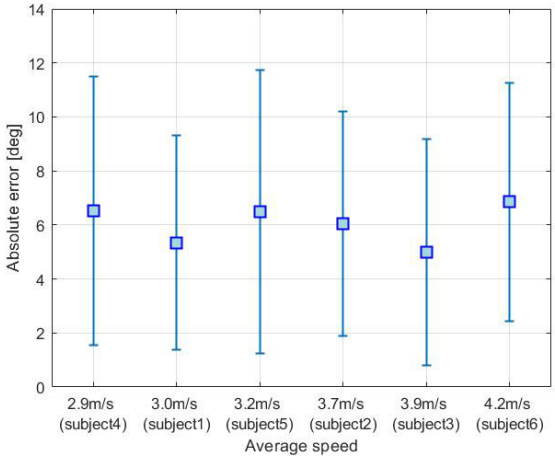


**FIGURE 10.** Error bars of the proposed method against the average speed of each subject.

CSV file. To exclude the error of transforming the inertial sensor outputs of the smartwatch from the body frame to the navigation frame, we used the AHRS solution provided by the MTi-680G, which has an accuracy of 0.2° RMS for roll and pitch and 0.5° RMS for yaw. The step detection algorithm in [39] was also used.

The true walking direction was calculated by differentiating the position obtained from the inertial navigation system (INS)/GNSS(RTK) solution of the MTi-680G at 1-second intervals, and the position was measured with an accuracy of CEP 1cm + 1ppm. Although the antenna is attached to the wrist, the wrist moves with the movement of the participant in close proximity to the body, and the changes caused by the wrist movement can be cancelled out by differentiating the change in position over 1-second period, thus the true walking direction can be calculated.

### B. VALIDATION OF THE COEFFICIENTS FOR MOTION DECOMPOSITION

We proceed to validate $c_{swing}$ and $c_{COM}$, which were introduced to facilitate the motion decomposition. The experiment was conducted on a straight 80m track. To verify whether $c_{swing}$ and $c_{COM}$ successfully reflect the decomposition of the motion, additional motions besides walking and running were included: only swinging the arms without walking and walking with the arms fixed to the body. It is anticipated that $c_{swing}$ should be close to 1 in the arm swing-only motion, while $c_{swing}$ should be close to 0 in the walking motion where the arms fixed to the body.

Fig. 8 and Table 2 compares the estimates of $c_{swing}$ and $c_{COM}$ for the four different motions. As anticipated, as shown in Table 2, the arm swing-only scenario yielded an average $c_{swing}$ estimate of 0.94, closely approaching 1. Conversely, when walking with the arms fixed to the body, the average $c_{swing}$ estimate was 0.03, closely approaching 0. The slight deviations from exact values of 1 and 0 for the coefficient can be attributed to modeling inaccuracies stemming from the kinematic modeling of the arm swing, sensor noise, and imperfect control over the motions of the participant. In the case of normal walking, the average estimate of $c_{swing}$ was 0.36, ranging between 0.3 and 0.42, and in the case of running, the average estimate of $c_{swing}$ was 0.26, ranging between 0.23 and 0.27. Based on the experimental results presented in Fig. 8 and Table 2, it can be concluded that our kinematic modeling of the arm swing accurately captures the nature of the motions, thus apt for estimating the actual walking direction.

### C. COMPARATIVE ANALYSIS ON RUNNING TRACK EXPERIMENT

To evaluate the performance of the proposed method, the participants engaged in running track experiment. The total distance of the experimental track is about 230m, which includes some curved sections. Table 3 summarizes the statistical analysis of RMPCA, LSM, WAISS, and the proposed method, including the mean error, standard deviation(std), and $90^{th}$ percentile. The $90^{th}$ percentile is the value corresponding to the $90^{th}$ percentile of the absolute estimation error when sorted in ascending order.

As shown in Table 3, the proposed method shows the best performance among the presented methods, achieving a mean error of 6.07°. It can be seen that the proposed method maintains the lowest error level compared to all other methods, as shown in Fig. 9, which compares the estimated walking direction and the corresponding estimation error for each method. Fig. 10 shows the mean error and standard deviation of the proposed method for each of the subjects running fast or slow at different speeds. Although the average speed of the subjects varies from 2.9m/s to 4.2m/s, the proposed method does not show significant performance differences for all subjects. This can be inferred as the running speed is synchronized with the amplitude of the arm swing, thus the coefficient $c_{swing}$ reflects their speed through the angular rate measurement and adjusts the direction vector.

**TABLE 3. Comparison of the walking direction estimation error on running track experiment.**

| Test User | RMPCA | | | LSM | | | WAISS | | | Proposed | | |
|---|---|---|---|---|---|---|---|---|---|---|---|---|
| | Mean [°] | Std [°] | $90^{th}$ percentile [°] | Mean [°] | Std [°] | $90^{th}$ percentile [°] | Mean [°] | Std [°] | $90^{th}$ percentile [°] | Mean [°] | Std [°] | $90^{th}$ percentile [°] |
| Subject1 | 21.10 | 5.92 | 28.03 | 14.69 | 5.68 | 22.99 | 14.88 | 4.58 | 20.52 | 5.34 | 3.97 | 10.87 |
| Subject2 | 20.47 | 4.46 | 26.14 | 12.05 | 4.42 | 17.91 | 16.65 | 3.87 | 21.20 | 6.04 | 4.16 | 11.80 |
| Subject3 | 20.01 | 6.56 | 28.14 | 13.69 | 7.58 | 21.46 | 18.17 | 6.21 | 25.15 | 4.97 | 4.18 | 9.72 |
| Subject4 | 18.52 | 6.88 | 27.03 | 16.16 | 4.66 | 21.53 | 16.41 | 5.18 | 23.03 | 6.52 | 4.96 | 13.69 |
| Subject5 | 19.53 | 7.33 | 28.20 | 13.49 | 7.72 | 22.23 | 15.62 | 4.26 | 21.10 | 6.48 | 5.24 | 13.13 |
| Subject6 | 22.40 | 5.66 | 29.84 | 14.99 | 6.80 | 23.59 | 14.52 | 6.92 | 23.98 | 6.84 | 4.42 | 14.12 |
| **Overall** | **20.15** | **6.27** | **27.95** | **14.15** | **6.45** | **21.81** | **16.11** | **5.45** | **22.52** | **6.07** | **4.66** | **12.20** |

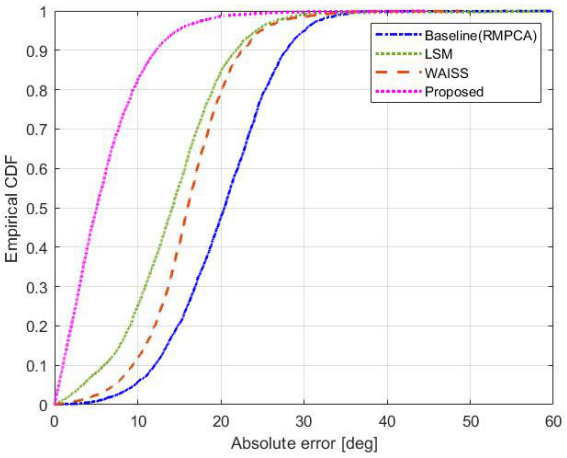


**FIGURE 11. Empirical cumulative distribution function (CDF) of absolute estimation error for each method.**

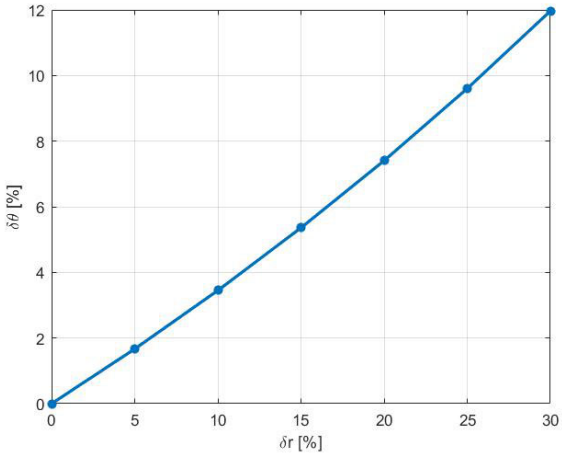


**FIGURE 12. Change in the estimated walking direction as *r* changes.**

Moreover, in terms of the $90^{th}$ percentile in Table 3, RMPCA gives 27.95°, LSM gives 21.81°, WAISS gives 22.52°, and the proposed method gives 12.20°. Given that the estimation error of the walking direction has a significant impact on positioning accuracy, maintaining an acceptable level of error is crucial, meaning even the $90^{th}$ percentile should be reasonably small. In this regard, the results show that the proposed method keeps the errors in check. The empirical cumulative distribution function (CDF) presented in Fig. 11 also shows that the proposed method is superior to the other methods.

The performance of the proposed method is affected by the parameter $r$, which is the linear distance from a point on the shoulder to the point where the sensor is mounted. In this experiment, the value of $r$ for each subject was measured directly beforehand and is presented in Table 1. As shown in Fig. 12, the ratio of the change in the estimated walking direction to the change in $r$ is 0.38 on average, indicating that the proposed method is not highly sensitive to $r$.

The results of the baseline method, RMPCA, suggest that this experimental conditions partially violate the underlying assumption of RMPCA. RMPCA assumes that the direction that maximizes the variance of the acceleration distribution aligns with the walking direction. While this assumption is appropriate for walking, it becomes disrupted during running, where the arm swings deviate from the actual walking direction. As shown in Fig. 9, RMPCA produces biased estimations characterized by the accumulation of non-forward acceleration resulting from the arm swing, thereby directly contributing to the estimation error. In contrast, the method proposed in this paper solves this problem and consistently demonstrates smaller estimation errors compared to RMPCA in Fig. 9.

LSM employs the concept of minimizing the angular rate in the walking direction. This concept is suitable for walking scenarios where the swing direction aligns with the walking direction. However, it becomes a significant source of estimation error during running, as the swing direction and walking direction deviate from each other. Meanwhile, WAISS requires an appropriate amount of data in a constrained setting to construct a GMM during the training phase. Furthermore, since the GMM is likely to vary for each individual and each motion, a personalized and finely segmented model is needed for accurate estimation of the walking direction [35]. In this experiment, the same participant generated a GMM using running data on a straight trajectory, but a separate GMM would be required for walking motion.

### D. COMPARATIVE ANALYSIS ON GENERAL SCENARIO

The participants performed walking and running on an extended and more challenging course in natural terrain. The total distance of the trajectory reaches approximately 800m. The 370-second scenario consists of two walking phases

**TABLE 4. Comparison of the walking direction estimation error on general scenario.**

| Test User | RMPCA | | | LSM | | | WAISS | | | Proposed | | |
|---|---|---|---|---|---|---|---|---|---|---|---|---|
| | Mean [°] | Std [°] | $90^{th}$ percentile [°] | Mean [°] | Std [°] | $90^{th}$ percentile [°] | Mean [°] | Std [°] | $90^{th}$ percentile [°] | Mean [°] | Std [°] | $90^{th}$ percentile [°] |
| Subject1 | 10.05 | 6.40 | 19.89 | 10.03 | 7.23 | 21.33 | 16.63 | 13.92 | 37.50 | 6.13 | 4.02 | 10.18 |
| Subject2 | 11.19 | 6.50 | 20.64 | 11.13 | 7.77 | 22.10 | 18.25 | 13.85 | 37.25 | 6.30 | 4.27 | 11.59 |
| Subject3 | 14.01 | 12.05 | 29.09 | 10.56 | 9.11 | 23.01 | 20.23 | 12.52 | 34.43 | 4.88 | 5.18 | 10.37 |
| Subject4 | 11.93 | 10.68 | 26.35 | 12.47 | 9.01 | 23.31 | 16.52 | 12.20 | 33.64 | 5.53 | 5.60 | 12.23 |
| Subject5 | 13.31 | 11.69 | 29.68 | 14.24 | 11.92 | 32.65 | 16.00 | 8.41 | 28.15 | 4.68 | 4.31 | 10.17 |
| Subject6 | 15.73 | 13.19 | 32.75 | 13.49 | 10.81 | 30.23 | 14.23 | 11.94 | 29.64 | 5.90 | 5.03 | 12.99 |
| **Overall** | **12.72** | **10.53** | **28.53** | **12.00** | **9.54** | **25.52** | **16.98** | **12.37** | **35.27** | **5.58** | **4.79** | **11.30** |

**TABLE 5. Overall performance by motion phase.**

| Phase | Mean error [°] | | | |
|---|---|---|---|---|
| | RMPCA | LSM | WAISS | Proposed |
| Walking | 5.17 | 5.52 | 7.45 | 4.77 |
| Running | 22.77 | 20.06 | 28.45 | 6.41 |

and two running phases. The walking phases are from 0 to 100 seconds and from 200 to 310 seconds, whereas the running phases are from 100 to 200 seconds and from 310 to 370 seconds.

Based on the analysis of human motion presented in Section III, the walking motion differs from running in that the arm swing is aligned with the walking direction. Given this characteristic, the walking direction for walking can be estimated from the results of the PCA on the acceleration given in Section IV-A alone. Thus, a module was incorporated to distinguish between walking and running prior to initiating the walking direction estimation process. This module examines the frequency of the magnitude of the acceleration measurements over a few steps [40] and classifies it as walking if the frequency is less than a certain threshold and as running if it is greater. Therefore, for walking, only Section IV-A, which involves PCA on the acceleration, is executed, while for running, the entire method is executed. The classifying module enhances the robustness of our method by ensuring accurate estimation when applied to general scenarios, such as running-walking-mixed situations.

Table 4 summarizes the estimation performance of each method in the general scenario of alternating walking and running. As shown in Table 4, the proposed method achieves a mean error of 5.58°, which is the best performance in comparison to the other methods. The proposed method also maintains the lowest error level of 11.30° in terms of the $90^{th}$ percentile. For a more detailed performance analysis, Table 5 shows the performance differences depending on the motion phase. It can be observed that all methods have similar estimation results in the two walking phases, whereas in the two running phases, the proposed method outperforms the other methods. In the running phase, the proposed method surpasses the other methods by more than 68%. These results can also be seen in Fig. 13 and Fig. 14, which present the walking direction estimation for subject1

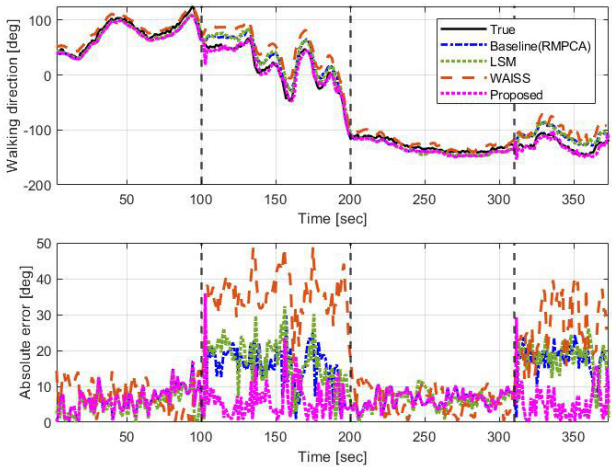


**FIGURE 13. Estimated walking direction and estimation error for subject1 in general scenario which consists of two walking phases and two running phases.**

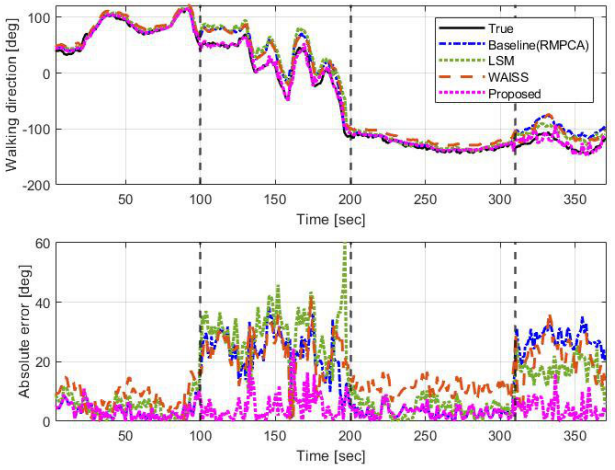


**FIGURE 14. Estimated walking direction and estimation error for subject5 in general scenario.**

and 5, respectively. This outperformance is not only owed to our accurate modeling of arm swing, but also to the inclusion of the classifying module explained in the previous paragraph, as it enabled the method to adapt to changing motion dynamics.

The baseline method, RMPCA, estimates the walking direction in the running phase as biased against the true walking direction due to the acceleration component caused

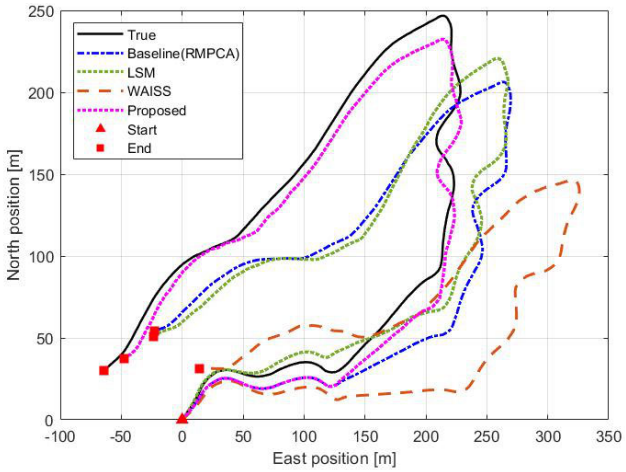


**FIGURE 15.** Pseudo-trajectory constructed by the estimated walking direction for subject1.

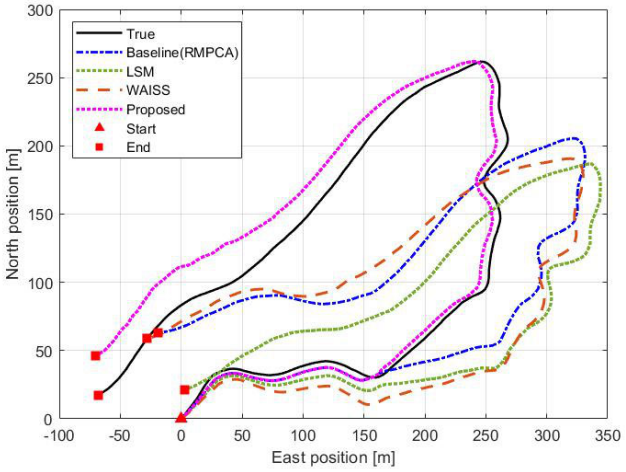


**FIGURE 16.** Pseudo-trajectory for subject5.

by the swing of the arm. It can be seen that the error of LSM increased in the running phase since the swing direction and the walking direction were not aligned during running. Meanwhile, for WAISS, a personalised GMM was created for each subject using their own walking data. As a result, WAISS performed comparably to other methods for walking, but had an increased error for running due to poor model fit. Furthermore, as shown in Fig. 13 and Fig. 14, the performance degradation due to model misfit can vary from person to person. This shows that WAISS is affected by the degree of granularity of the GMM, both individual and motion.

Finally, Fig. 15 and Fig. 16 present the pseudo-trajectory derived from the estimated walking direction by each method for subject1 and 5, respectively. The step length was calculated using the step detection time and walking speed, assumed to be 1.4m/s for walking and 3m/s for running. Notably, the proposed method follows the true trajectory more accurately than the other methods. In Table 6, the RMSE of the pseudo-trajectory estimated by the proposed method

**TABLE 6.** Overall positional accuracy for pseudo-trajectory.

| | RMPCA | LSM | WAISS | Proposed |
|---|---|---|---|---|
| RMSE [m] | 61.43 | 59.48 | 84.07 | 17.44 |
| Final* [%] | 8.58 | 8.00 | 9.74 | 2.42 |

* Final = (final position error / total distance) * 100

for all subjects is 17.44m, and the final position error with respect to the total distance is 2.42%, which is the smallest error. Therefore, the proposed method has broadened the applicability of the PCA-based walking direction estimation method by accommodating fundamental human motions, namely walking and running.

## VI. CONCLUSION

This paper proposed a novel walking direction estimation method that effectively isolates movement of the center of mass of the body from the swing movement of the arm, an inevitable misalignment problem when using smartwatch data collected while running. The method employs a combination of PCAs for acceleration and angular rate, alongside motion decomposition based on human gait kinematics. The performance of the proposed method was evaluated through real-world experiments, particularly with general scenario involving both walking and running to ensure the broad applicability of the method. While the experiments were conducted with a smartwatch-wearing participants, the method can also be applied to other platforms held in the hand, such as smartphones, to capture the swing motion of the arm. Furthermore, although the experiments were conducted outdoors to obtain true walking direction using GNSS(RTK) information, the method can be equally effective indoors as the inertial sensor itself does not rely on external infrastructure.

## APPENDIX
## DERIVATION OF THE RELATION BETWEEN THE COEFFICIENTS

The relationship between $c_{COM}$ and $c_{swing}$ given in (8) in Section IV is derived from the fact that $\boldsymbol{u}$ is a unit vector in (1). Expressing (1) in terms of its components, we have

$$\boldsymbol{u} = \begin{bmatrix} u_N \\ u_E \end{bmatrix} = \begin{bmatrix} c_C u_{C,N} + c_s u_{s,N} \\ c_C u_{C,E} + c_s u_{s,E} \end{bmatrix} \tag{17}$$

where $N, E$ are the North and East axes, respectively, and the subscripts $C$, $s$ are $COM$ and $swing$, respectively. Since $\boldsymbol{u}$ is a unit vector, we have

$$||\boldsymbol{u}||_2 = \left\| \begin{bmatrix} u_N \\ u_E \end{bmatrix} \right\|_2 = 1. \tag{18}$$

By definition of $l^2$-norm,

$$\left\| \begin{bmatrix} u_N \\ u_E \end{bmatrix} \right\|_2 = \sqrt{u_N^2 + u_E^2} = 1 \tag{19}$$

where

$$u_N^2 = c_C^2 u_{C,N}^2 + c_s^2 u_{s,N}^2 + 2c_C c_s u_{C,N} u_{s,N} \quad (20)$$

$$u_E^2 = c_C^2 u_{C,E}^2 + c_s^2 u_{s,E}^2 + 2c_C c_s u_{C,E} u_{s,E}. \quad (21)$$

Since $||\boldsymbol{u}_C||_2^2 = u_{C,N}^2 + u_{C,E}^2 = 1$, $||\boldsymbol{u}_s||_2^2 = u_{s,N}^2 + u_{s,E}^2 = 1$, $\boldsymbol{u}_C \cdot \boldsymbol{u}_s = u_{C,N}u_{s,N} + u_{C,E}u_{s,E} = ||\boldsymbol{u}_C||_2||\boldsymbol{u}_s||_2 \cos\alpha = \cos\alpha$, we have

$$c_C^2 + c_s^2 + 2c_C c_s \cos\alpha = 1 \quad (22)$$

where $\alpha$ is the angle between $\boldsymbol{u}_C$ and $\boldsymbol{u}_s$. If we solve (22) for $c_C$,

$$c_C = -c_s \cos\alpha + \sqrt{1 - c_s^2 \sin^2\alpha}. \quad (23)$$

Hence, the relation between the coefficients is derived as follows.

$$c_C + c_s = c_s(1 - \cos\alpha) + \sqrt{1 - c_s^2 \sin^2\alpha}. \quad (24)$$

Considering the condition that occurs in the case of running, the sum of the two coefficients can be approximated as

$$c_C + c_s \approx 1 \quad (25)$$

which confirms (8).

## REFERENCES

[1] V. F. Miramá, L. E. Díez, A. Bahillo, and V. Quintero, "A survey of machine learning in pedestrian localization systems: Applications, open issues and challenges," *IEEE Access*, vol. 9, pp. 120138–120157, 2021.
[2] H. Li, H. Liu, Z. Li, C. Li, Z. Meng, N. Gao, and Z. Zhang, "Adaptive threshold based ZUPT for single IMU enabled wearable pedestrian localization," *IEEE Internet Things J.*, vol. 10, no. 13, pp. 11749–11760, Jul. 2023.
[3] Z. Qin, Z. Meng, Z. Li, N. Gao, Z. Zhang, Q. Meng, and D. Zhen, "Compensating the NLoS occlusion errors of UWB for pedestrian localization with MIMU," *IEEE Sensors J.*, vol. 23, no. 11, pp. 12146–12158, Jun. 2023.
[4] R. Sun, L. Fu, Q. Cheng, K.-W. Chiang, and W. Chen, "Resilient pseudorange error prediction and correction for GNSS positioning in urban areas," *IEEE Internet Things J.*, vol. 10, no. 11, pp. 9979–9988, Jun. 2023.
[5] C. Chen, G. Chang, N. Zheng, and T. Xu, "GNSS multipath error modeling and mitigation by using sparsity-promoting regularization," *IEEE Access*, vol. 7, pp. 24096–24108, 2019.
[6] Z. Hao, J. Dang, W. Cai, and Y. Duan, "A multi-floor location method based on multi-sensor and WiFi fingerprint fusion," *IEEE Access*, vol. 8, pp. 223765–223781, 2020.
[7] R. Wang, H. Luo, Q. Wang, Z. Li, F. Zhao, and J. Huang, "A spatial–temporal positioning algorithm using residual network and LSTM," *IEEE Trans. Instrum. Meas.*, vol. 69, no. 11, pp. 9251–9261, Nov. 2020.
[8] R. Wang, Z. Li, H. Luo, F. Zhao, W. Shao, and Q. Wang, "A robust Wi-Fi fingerprint positioning algorithm using stacked denoising autoencoder and multi-layer perceptron," *Remote Sens.*, vol. 11, no. 11, p. 1293, May 2019.
[9] R. Ali, R. Liu, A. Nayyar, B. Qureshi, and Z. Cao, "Tightly coupling fusion of UWB ranging and IMU pedestrian dead reckoning for indoor localization," *IEEE Access*, vol. 9, pp. 164206–164222, 2021.
[10] N. Yu, X. Zhan, S. Zhao, Y. Wu, and R. Feng, "A precise dead reckoning algorithm based on Bluetooth and multiple sensors," *IEEE Internet Things J.*, vol. 5, no. 1, pp. 336–351, Feb. 2018.
[11] J. Lai, C. Luo, J. Wu, J. Li, J. Wang, J. Chen, G. Feng, and H. Song, "TagSort: Accurate relative localization exploring RFID phase spectrum matching for Internet of Things," *IEEE Internet Things J.*, vol. 7, no. 1, pp. 389–399, Jan. 2020.
[12] R. Harle, "A survey of indoor inertial positioning systems for pedestrians," *IEEE Commun. Surveys Tuts.*, vol. 15, no. 3, pp. 1281–1293, 3rd Quart., 2013.
[13] H. Ju, S. Y. Park, and C. G. Park, "A smartphone-based pedestrian dead reckoning system with multiple virtual tracking for indoor navigation," *IEEE Sensors J.*, vol. 18, no. 16, pp. 6756–6764, Aug. 2018.
[14] L. Pei, D. Liu, D. Zou, R. Lee Fook Choy, Y. Chen, and Z. He, "Optimal heading estimation based multidimensional particle filter for pedestrian indoor positioning," *IEEE Access*, vol. 6, pp. 49705–49720, 2018.
[15] R. Mahony, T. Hamel, and J.-M. Pflimlin, "Nonlinear complementary filters on the special orthogonal group," *IEEE Trans. Autom. Control*, vol. 53, no. 5, pp. 1203–1218, Jun. 2008.
[16] S. O. H. Madgwick, A. J. L. Harrison, and R. Vaidyanathan, "Estimation of IMU and MARG orientation using a gradient descent algorithm," in *Proc. IEEE Int. Conf. Rehabil. Robot.*, Jun. 2011, pp. 1–7.
[17] J. G. Martins, M. R. Petry, and A. P. Moreira, "Assessment of the influence of magnetic perturbations and dynamic motions in a commercial AHRS," in *Proc. IEEE Int. Conf. Auto. Robot Syst. Competitions (ICARSC)*, Apr. 2023, pp. 175–180.
[18] S. A. Hoseinitabatabaei, A. Gluhak, R. Tafazolli, and W. Headley, "Design, realization, and evaluation of uDirect—An approach for pervasive observation of user facing direction on mobile phones," *IEEE Trans. Mobile Comput.*, vol. 13, no. 9, pp. 1981–1994, Sep. 2014.
[19] Z.-A. Deng, G. Wang, Y. Hu, and D. Wu, "Heading estimation for indoor pedestrian navigation using a smartphone in the pocket," *Sensors*, vol. 15, no. 9, pp. 21518–21536, Aug. 2015.
[20] M. Uddin, A. Gupta, K. Maly, T. Nadeem, S. Godambe, and A. Zaritsky, "SmartSpaghetti: Accurate and robust tracking of Human's location," in *Proc. IEEE-EMBS Int. Conf. Biomed. Health Informat. (BHI)*, Jun. 2014, pp. 129–132.
[21] M. Kourogi and T. Kurata, "A method of pedestrian dead reckoning for smartphones using frequency domain analysis on patterns of acceleration and angular velocity," in *Proc. IEEE/ION Position, Location Navigat. Symp. (PLANS)*, May 2014, pp. 164–168.
[22] J. Kuang, X. Niu, and X. Chen, "Robust pedestrian dead reckoning based on MEMS-IMU for smartphones," *Sensors*, vol. 18, no. 5, p. 1391, May 2018.
[23] K. Kunze, P. Lukowicz, K. Partridge, and B. Begole, "Which way am I facing: Inferring horizontal device orientation from an accelerometer signal," in *Proc. Int. Symp. Wearable Comput.*, Sep. 2009, pp. 149–150.
[24] R. Leonardo, G. Rodrigues, M. Barandas, P. Alves, R. Santos, and H. Gamboa, "Determination of the walking direction of a pedestrian from acceleration data," in *Proc. Int. Conf. Indoor Positioning Indoor Navigat. (IPIN)*, Sep. 2019, pp. 1–6.
[25] D. Liu, L. Pei, J. Qian, L. Wang, P. Liu, Z. Dong, S. Xie, and W. Wei, "A novel heading estimation algorithm for pedestrian using a smartphone without attitude constraints," in *Proc. 4th Int. Conf. Ubiquitous Positioning, Indoor Navigat. Location Based Services (UPINLBS)*, Nov. 2016, pp. 29–37.
[26] X. Lou, L. Zhi, and J. Fang, "An algorithm which can obtain the global walking direction," in *Proc. 12th Int. Conf. Fuzzy Syst. Knowl. Discovery (FSKD)*, Aug. 2015, pp. 2619–2624.
[27] A. Manos, T. Hazan, and I. Klein, "Walking direction estimation using smartphone sensors: A deep network-based framework," *IEEE Trans. Instrum. Meas.*, vol. 71, pp. 1–12, 2022.
[28] N. Roy, H. Wang, and R. Roy Choudhury, "I am a smartphone and I can tell my user's walking direction," in *Proc. 12th Annu. Int. Conf. Mobile Syst., Appl., services*, Jun. 2014, pp. 329–342.
[29] M. F. Shaikh, Z. Salcic, and K. I. Wang, "A novel accelerometer-based technique for robust detection of walking direction," *IEEE Trans. Biomed. Eng.*, vol. 65, no. 8, pp. 1740–1747, Aug. 2018.
[30] C. Combettes and V. Renaudin, "Walking direction estimation based on statistical modeling of human gait features with handheld MIMU," *IEEE/ASME Trans. Mechatronics*, vol. 22, no. 6, pp. 2502–2511, Dec. 2017.
[31] J. Perul and V. Renaudin, "HEAD: SmootH Estimation of wAlking direction with a handheld device embedding inertial, GNSS, and magnetometer sensors," *Annu. Navigat.*, vol. 67, no. 4, pp. 713–726, 2020.
[32] X. Yang, B. Huang, and Q. Miao, "A step-wise algorithm for heading estimation via a smartphone," in *Proc. Chin. Control Decis. Conf. (CCDC)*, May 2016, pp. 4598–4602.
[33] C. Combettes and V. Renaudin, "Comparison of misalignment estimation techniques between handheld device and walking directions," in *Proc. Int. Conf. Indoor Positioning Indoor Navigat. (IPIN)*, Oct. 2015, pp. 1–8.

[34] J. Perul and V. Renaudin, "Building individual inertial signals models to estimate PDR walking direction with smartphone sensors," in *Proc. Int. Conf. Indoor Positioning Indoor Navigat. (IPIN)*, Sep. 2018, pp. 1–8.
[35] J. Perul and V. Renaudin, "Learning individual models to estimate the walking direction of mobile phone users," *IEEE Sensors J.*, vol. 19, no. 24, pp. 12306–12315, Dec. 2019.
[36] P. G. Adamczyk, S. H. Collins, and A. D. Kuo, "The advantages of a rolling foot in human walking," *J. Experim. Biol.*, vol. 209, no. 20, pp. 3953–3963, Oct. 2006.
[37] S. M. Bruijn, O. G. Meijer, P. J. Beek, and J. H. van Dieën, "The effects of arm swing on human gait stability," *J. Experim. Biol.*, vol. 213, no. 23, pp. 3945–3952, Dec. 2010.
[38] S. H. Collins, P. G. Adamczyk, and A. D. Kuo, "Dynamic arm swinging in human walking," *Proc. Roy. Soc. B, Biol. Sci.*, vol. 276, no. 1673, pp. 3679–3688, Oct. 2009.
[39] S. Park, J. H. Lee, and C. G. Park, "Robust pedestrian dead reckoning for multiple poses in smartphones," *IEEE Access*, vol. 9, pp. 54498–54508, 2021.
[40] Y. Chen and C. Shen, "Performance analysis of smartphone-sensor behavior for human activity recognition," *IEEE Access*, vol. 5, pp. 3095–3110, 2017.

**JAE WOOK PARK** received the B.S. degree from the Department of Physics, University of Seoul, Seoul, South Korea, in 2022. He is currently pursuing the M.S. degree with the Department of Aerospace Engineering, Seoul National University, Seoul.

His research interests include inertial navigation systems and pedestrian dead reckoning.

**JAE HONG LEE** (Student Member, IEEE) received the B.S. degree from the School of Mechanical and Electrical Control Engineering, Handong Global University, in 2017, and the M.S. degree from the Department of Mechanical and Aerospace Engineering, Seoul National University, Seoul, South Korea, in 2019, where he is currently pursuing the Ph.D. degree.

His research interests include pedestrian dead reckoning and inertial navigation systems.

**JUNU PARK** received the B.S. degree from the Department of Aerospace Engineering, Seoul National University, Seoul, South Korea, in 2022, where he is currently pursuing the M.S. degree.

His research interests include inertial navigation systems and pedestrian dead reckoning.

**CHAN GOOK PARK** (Member, IEEE) received the B.S., M.S., and Ph.D. degrees in control and instrumentation engineering from Seoul National University, Seoul, South Korea, in 1985, 1987, and 1993, respectively.

He was a Postdoctoral Fellow with Prof. J. L. Speyer about peak seeking control for formation flight with the University of California at Los Angeles, Los Angeles, CA, USA, in 1998. From 1994 to 2003, he was an Associate Professor with Kwangwoon University, Seoul. In 2003, he joined as a Faculty Member with the School of Mechanical and Aerospace Engineering, Seoul National University, where he is currently a Professor. In 2009, he was a Visiting Scholar with the Department of Aerospace Engineering, Georgia Institute of Technology, Atlanta, GA, USA. His current research interests include advanced filtering techniques, high precision inertial navigation systems (INSs), visual-inertial odometry (VIO), INS/global navigation satellite system(GNSS)/image-based navigation(IBN) integration, and smartphone-based/foot-mounted pedestrian dead reckoning (PDR) systems. He served as the Chair for the IEEE AES Korea Chapter until 2009.